Bioorganic Chemistry 163 (2025) 108789

Contents lists available at ScienceDirect

Bioorganic Chemistry

journal homepage: www.elsevier.com/locate/bioorg

New rhodium(III)-triphenylphosphine complexes with 5-halogenate-8-hydroxyquinoline as ligands: synthesis, characterization, cytotoxicity, and mechanism of action

Zhen-Feng Wang [a,b], Xiao-Qiong Huang [c], Run-Chun Wu [c], Shu-Hua Zhang [a,b,*], Guangzhao Li [a,**]

[a] College of Chemistry, Guangdong University of Petrochemical Technology, Maoming, Guangdong, PR China
[b] Guangxi Key Laboratory of Electrochemical and Magnetochemical Functional Materials, Guilin University of Technology, Guilin, PR China
[c] Guangxi Key Lab of Agricultural Resources Chemistry and Biotechnology, College of Chemistry and Food Science, Yulin Normal University, 1303 Jiaoyudong Road, Yulin 537000, PR China

ARTICLE INFO

Keywords:
Rhodium(III) complexes
5-halogenate-8-hydroxyquinoline
Triphenylphosphine
Mitophagy
Apoptosis

ABSTRACT

The incorporation of triphenylphosphine (PPh_3) can enhance the antiproliferative activity of complexes. Herein, four Rh(III) complexes **GUPT1-GUPT4** were synthesized. **GUPT4** exhibited stronger anticancer activity than HGU, cisplatin, and **GUPT1**–**GUPT3** against human non-small cell lung A549 and its cisplatin-resistant A549 cell line (CR-A549), with IC_{50} values of 6.73 ± 0.41 and 5.11 ± 0.16 μM, respectively. The antiproliferative activity of the four Rh^{III} complexes increased with different 5-substituted ligands in the following order: —H (**GUPT1**) < —Br (**GUPT2**) < —Cl (**GUPT3**) < —F (**GUPT4**). **GUPT3** and **GUPT4** induce CR-A549 mitochondrial autophagy and ATP blockade, leading to apoptosis. In addition, the inhibition rate of **GUPT4** on A549 was 39.1 %, showing potential antitumor efficacy. Thus, **GUPT3** and **GUPT4** can be considered as promising non-Pt drug candidates for lung cancer treatment.

1. Introduction

Platinum-based drugs, such as cisplatin and its clinically successful derivatives, have been widely used to treat various types of cancers, with their success driving the development of new Pt(II/IV) and non-Pt(II/IV) chemotherapeutics that can overcome drug resistance with minimal side effects [1–4]. Meanwhile, Rhodium complexes are a class of metal compounds with unique and diverse biological activities, especially in the field of anti-cancer (including overcoming drug resistance and light activation strategies) show great potential. Its light response characteristics (photodynamic therapy and photoactivated chemotherapy) are the most concerned and characteristic research directions[5–14]. In line with this, various rhodium(II/III) complexes with different organic ligands such as thiabendazole−/benzimidazole-based derivatives [5a], benzo[*i*]dipyrido[3,2-a,2′,3′-c]phenazine [6], 1,3-dimethylbenzimidazolium iodide or 1,3-dibenzylbenzimidazolium bromide [7], N-(3-halogen-phenyl)picolinamide ligands [8], 2-phenylpyridinate derivatives [9], 1,2,4-triazole [10], 2-pyridinecarbothioamide (PCA) ligand [11], triazolopyrimidines [12], pyrazolopyrimidine derivatives [13], and sulfonated iminopyridine ligands [14] have been explored for their anticancer and anti-inflammatory activities. However, the antiproliferative mechanisms of rhodium(III) derivatives remain poorly understood, limiting their application in clinical chemotherapy.

A series of 8-hydroxyquinoline (HGU) metal derivatives have been developed as antiproliferative agents and extensively studied by several research groups [15–25]. In particular, rhodium(III) complexes [26] featuring various ligands, such as 8-hydroxyquinoline or 5-bromo-8-hydroxyquinoline [27], 8-hydroxyquinoline-5-sulfonate or 7-(1-piperidinylmethyl)-8-hydroxyquinoline [28], (*S*)-5-chloro-7-((proline-1-yl)methyl)8-hydroxyquinoline derivatives [29], and 8-hydroxy-2-methylquinoline [30], have demonstrated remarkable anticancer activity.

Highlights PPh_3 is a ligand with strong σ-donating, moderate π-accepting and large steric hindrance. Its bonding to metals involves the synergy of σ-giving and feedback π-bonding. Strong σ-giving affects the electron density of the metal, which in turn affects its redox, reactivity, and ligand exchange rate.[31–35] at the same time, π-acceptance

* Corresponding author at: College of Chemistry, Guangdong University of Petrochemical Technology, Maoming, Guangdong, PR China.
** Corresponding author.
E-mail addresses: zhangshuhua@gdupt.edu.cn (S.-H. Zhang), gzli666@gdupt.edu.cn (G. Li).

https://doi.org/10.1016/j.bioorg.2025.108789
Received 22 May 2025; Received in revised form 17 July 2025; Accepted 21 July 2025
Available online 25 July 2025

helps stabilize metal centers in low oxidation states. On the other hand, huge steric hindrance is its most prominent feature, which protects the metal center (improves kinetic inertness), controls coordination geometry and ligand dissociation, and profoundly affects the binding mode and efficiency of complexes with biological targets (such as DNA). [31–35] meanwhile, hydrophobic phenyl groups significantly increase lipid solubility and promote cellular uptake. Therefore, when designing metal complexes with specific biological activities, choosing PPh_3 or modifying their structure (such as introducing different substituents to change electronic effects and steric hindrance) is a key strategy for regulating the physical and chemical properties of drugs (solubility, stability), pharmacokinetics (absorption, distribution) and pharmacodynamics (target binding, reactivity).[31–35] the balance between its electronic and spatial properties is critical to the final biological activity. Additionally, the antiproliferative activity of several metal complexes increased with the introduction of triphenylphosphine (—PPh_3) and halogen (—X) co-ligands [15e,36–38]; however, their water solubility was not significantly improved [15e,36–38]. In this context, the high antiproliferative activity of GUPT1–GUPT4, which combine HGU1–HGU4 with PPh_3, has yet to be reported and remains largely unexplored [20e,36–38]

Thus, we designed and synthesized four rhodium(III)-triphenylphosphine complexes **GUPT1–GUPT4** with high anticancer activity. These compounds, namely [Rh(GU1)$(PPh_3)_2Cl_2$] (**GUPT1**), [Rh(GU2)$(PPh_3)_2Cl_2$] (**GUPT2**), [Rh$(GU3)_2(PPh_3)$Cl] (**GUPT3**), and [Rh$(GU4)_2(PPh_3)$Cl] (**GUPT4**), (HGU = 5-R-8-hydroxyquinoline, R = H, HGU1; R = Br, HGU2; R = Cl, HUG3, R = F, HGU4), were derived from 8-hydroxyquinoline derivates (HGU1–HGU4) and tris(triphenylphosphine)rhodium(I) chloride ($(PPh_3)_3$RhCl). In addition, the cytotoxicity and antitumor mechanisms of **GUPT1–GUPT4** against A549 and CR-A549 tumor cells were evaluated.

2. Results and discussion

2.1. Synthesis and characterization

The reactions of the precursor ($(PPh_3)_3$RhCl, CAS number: 14694–95-2) with the HGU1–HGU4 ligands in a mixture of methanol, dichloromethane, and triethylamine at 65 °C for 1.0 day and subsequently at 80 °C for 3.0 days in a 15-mL high-temperature resistant tube afforded the target compounds **GUPT1–GUPT4** in isolated yields of 40.8–60.5 % (Scheme 1). In addition, **GUPT1–GUPT4** were characterized by electrospray ionization mass spectrometry (Figs. S1 and S2), ^{1}H NMR (Figs. S3–S5), elemental analysis, and X-ray diffraction analysis (Figs. 1,2 Fig. S6 and Tables 1–2). The structures of **GUPT1-GUPT4** are striking similar except that they have different amounts of GU, PPh_3

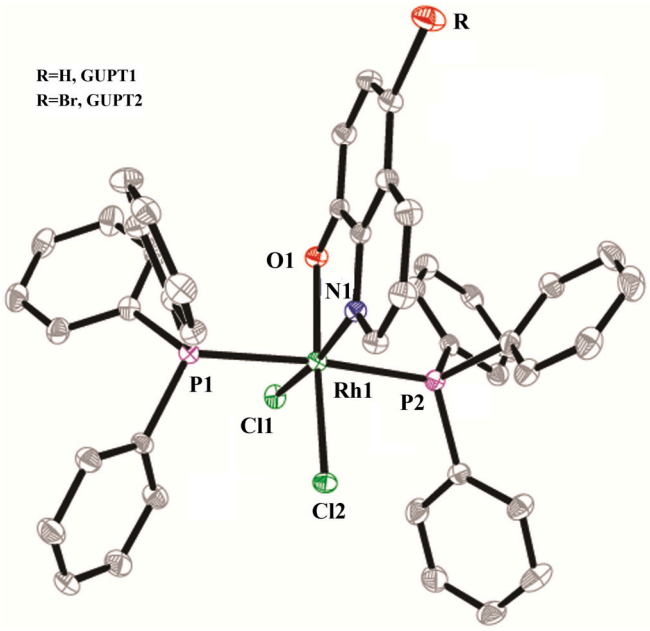

Fig. 1. Crystal structures of **GUPT1** and **GUPT2** with the H atoms were omitted for clarity. Displacement ellipsoids are drawn at the 30 % probability level.

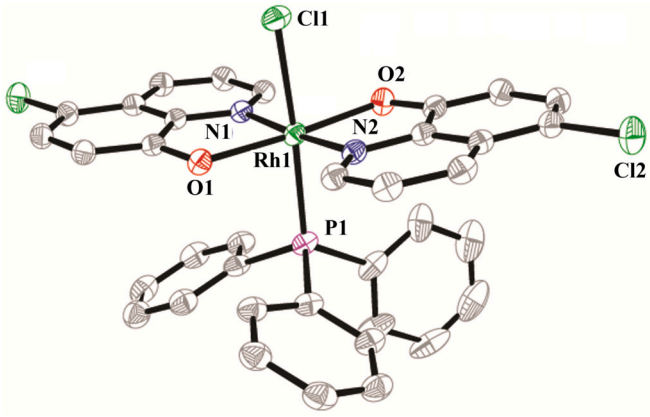

Fig. 2. Crystal structure of **GUPT3** with the H atoms were omitted for clarity. Displacement ellipsoids are drawn at the 30 % probability level.

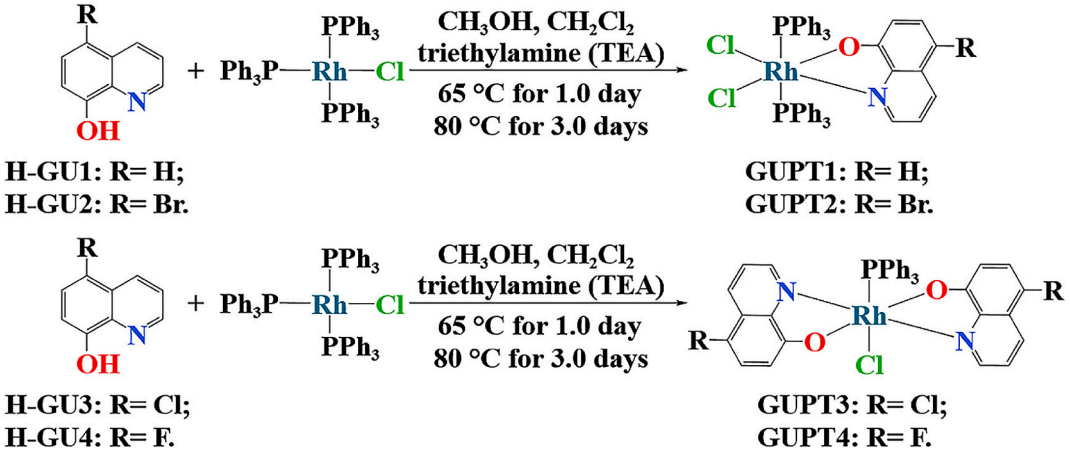

Scheme 1. Synthesis of **GUPT1–GUPT4**.

Table 1
Crystallographic data for **GUPT1–GUPT4.**

Complexes	GUPT1	GUPT2	GUPT3	GUPT4
Formula	$C_{45}H_{36}Cl_2NOP_2Rh$	$C_{45}H_{35}BrCl_2NOP_2Rh$	$C_{36}H_{25}Cl_3N_2O_2PRh$	$C_{36}H_{25}ClF_2N_2O_2PRh$
Mr	842.50	921.40	757.81	724.91
Crystal size(mm)	0.39 × 0.21 × 0.12	0.22 × 0.21 × 0.18	0.26 × 0.25 × 0.19	0.23 × 0.20 × 0.18
Crystal system	Monoclinic	Monoclinic	Triclinic	Monoclinic
Space group	$P2_1/c$	$C2/c$	P-1	$P2_1/n$
a/Å	15.471(1)	24.7490(4)	11.517(1)	12.345(1)
b/Å	20.319(1)	12.2019(2)	11.612(1)	15.913(8)
c/Å	24.651(1)	26.4634(3)	13.389(1)	16.713(1)
α/°	90	90	76.915(1)	90
β/°	101.800(2)	106.366(1)	66.095(1)	104.625(6)
γ/°	90	90	77.051(1)	90
Volume/Å^3	7585.0(6)	7667.7(2)	1576.69(10)	3176.6(3)
Z	8	8	2	4
F(000)	3440	3712	764	1464
D_C(g/cm^3)	1.476	1.596	1.596	1.516
μ/mm^{-1}	0.713	7.187	0.884	0.720
2θ range (°)	4.95–121.79	6.96–151.65	4.10–50.20	4.72–50.20
Ref. Meas./indep.	101,842/17384	25,857/7357	35,688/5541	11,254/5645
Obs.Ref.[$I \geq 2\sigma(I)$]	14,890	6654	4902	4110
R_{int}	0.0624	0.0436	0.0293	0.0552
R_1 [$I \geq 2\sigma(I)$][a]	0.0467	0.0316	0.0356	0.0521
ωR_2 (all data)[b]	0.1180	0.0864	0.0818	0.1650
Goof	1.002	1.006	1.000	1.138
Δρ(max, min) (eÅ^{-3})	1.027, −1.459	0.516,-0.653	1.558, −0.482	0.906,-1.064

[a] $R_1 = \Sigma||F_o| - |F_c||/\Sigma|F_o|$.
[b] $wR_2 = [\Sigma w(|F_o^2| - |F_c^2|)^2/\Sigma w(|F_o^2|)^2]^{1/2}$.

Table 2
Selected bond lengths (Å) and angles (°) for **GUPT1–GUPT4.**

Complexes	GUPT1	GUPT2	GUPT3	GUPT4
Rh1—O1	2.025(2)	2.038(2)	2.039(2)	2.030(4)
Rh1—N1	2.037(3)	2.057(2)	2.012(3)	2.084(4)
Rh1—X2	2.3554(9)	2.3629(6)	2.022(2)	2.027(3)
Rh1—Cl1	2.3613(8)	2.3550(6)	2.3923(9)	2.355(1)
Rh1—P1	2.3942(9)	2.4022(7)	2.3071(9)	2.292(1)
Rh1—Y2	2.3867(8)	2.3919(7)	2.019(3)	2.011(4)
O1—Rh1—N1	82.66(10)	81.61(7)	82.06(10)	81.19(17)
O1—Rh1—X2	87.71(7)	173.90(5)	176.18(10)	170.47(15)
N1—Rh1—X2	170.35(8)	92.40(6)	96.63(10)	92.35(16)
O1—Rh1—Cl1	175.96(7)	89.82(5)	89.12(7)	93.19(12)
N1—Rh1—Cl1	93.30(8)	171.40(6)	89.14(8)	88.15(13)
X2—Rh1—Cl1	96.32(3)	96.18(2)	87.27(8)	93.60(11)
O1—Rh1—Y2	89.06(7)	92.10(6)	98.98(10)	90.09(17)
N1—Rh1—Y2	89.29(8)	92.40(6)	176.02(11)	90.21(17)
X2—Rh1—Y2	89.80(3)	87.10(2)	82.08(10)	82.89(16)
Cl1—Rh1—Y2	90.80(3)	87.28(2)	87.04(8)	176.06(13)
O1—Rh1—P1	91.83(7)	91.29(6)	86.53(7)	95.39(12)
N1—Rh1—P1	89.73(8)	92.40(6)	91.65(8)	175.40(13)
X2—Rh1—P1	91.34(3)	90.15(2)	97.11(8)	91.40(11)
Cl1—Rh1—P1	88.24(3)	86.81(2)	175.42(4)	88.97(5)
Y2—Rh1—P1	178.58(3)	173.17(2)	92.25(8)	92.89(12)

GUPT1: X = Cl, Y = P, **GUPT2**:X = Cl, Y = P; **GUPT3**: X = O, Y = N, **GUPT3**: X = O, Y = N.

ligands, Cl ions or different directions of extension of the ligands in the space. Therefore, only **GUPT2** is analyzed here.

Single-crystal X-ray diffraction analysis reveals that **GUPT2** belongs to the monoclinic space group *C*2/*c*, and it consists of one Rh^{III} atom, two PPh_3 ligands, one GU2 ligand and two counter-anion Cl^- ions. The Rh1 atom in **GUPT2** is six-coordinated to P atom (P1, P2) in two PPh_3 ligands (Rh1—P1 = 2.3942(9) Å; Rh1—P2 = 2.3867(8) Å), and to one N, one O atom belonging to one GU2 ligand (Rh1—O1, 2.025(2) Å; Rh1—N1, 2.037(3) Å), and to two Cl ions (Rh1—Cl1, 2.3613(8) Å; Rh1—Cl2, 2.3554(9) Å), in line with the results obtained for previously reported rhodium compounds [26–30,39,40], resulting in a slightly distorted octahedron geometry (Fig. 1, Table 2). The **GUPT2** molecule exists intramolecular hydrogen bond (C29—H29···O1, 3.111(1) Å) which further formed 3D network through abundant Br···Br interaction (Br1···Br1[a], 3.858(2) Å, symmetry code: (a) 1 − *x*, 2 − *y*, 1 − *z*.) and C—H···Cl hydrogen bonds (C43—H43···Cl1[b], 3.520(2) Å; symmetry code: (b) 1 − *x*, *y*, 0.5 − *z*. Fig. S7). Furthermore, the CCDC deposition numbers for **GUPT1–GUPT4** are 2,325,993–2,325,996, respectively.

2.2. Cytotoxicity against cancer cells

The cytotoxic activity of **GUPT1–GUPT4** was evaluated against non-malignant Human Embryonic Kidney (HEK293), cancerous human non-small cell lung A549, and cisplatin-resistant CR-A549 human cell lines using CCK-8 assays [15e,41,42]. In CR-A549 cells, **GUPT4** exhibited the highest antitumor potency (IC_{50} = 5.11 ± 0.16 μM), significantly outperforming HGU1–HGU4 ligands (>50 μM), $(PPh_3)_3RhCl$ (>50 μM), cisplatin (>50 μM), **GUPT1** (14.59 ± 0.26 μM), **GUPT2** (12.07 ± 0.44 μM), and **GUPT3** (8.74 ± 1.02 μM) (Table 3). The antiproliferative activities of the rhodium(III)–triphenylphosphine complexes against A549 cancer cells also followed the order: **GUPT4** > **GUPT3** > **GUPT2** > **GUPT1** > cisplatin ≈ HGU1–HGU4 ligands ≈ $(PPh_3)_3RhCl$. **GUPT4** demonstrated greater potency than previously reported rhodium(III)–8-hydroxyquinoline derivatives [26–30] in CR-A549 cancer cells (Table 3). Interestingly, **GUPT1–GUPT4** showed promising selectivity toward CR-A549 cells (Table 3), exhibiting a 3.4–9.8-fold lower cytotoxicity against HEK293 noncancerous cells than cisplatin. This suggests that their antiproliferative effects may involve a cell death/apoptosis mechanism different from that of cisplatin. Among the rhodium(III)-8-

Table 3
Cytotoxicity (IC_{50}, μM) of **GUPT1–GUPT4** in HEK293, A549, and CR-A549 cell lines after 48 h treatment (CCK-8 assay).

	CR-A549	A549	HEK293
HGU1	>50	>50	>50
GUPT1	14.59 ± 0.26	25.09 ± 0.94	>50
HGU2	>50	>50	>50
GUPT2	12.07 ± 0.44	19.35 ± 0.88	>50
HGU3	>50	>50	>50
GUPT3	8.74 ± 1.02	10.36 ± 0.11	>50
HGU4	>50	>50	>50
GUPT4	5.11 ± 0.16	6.73 ± 0.41	>50
$(PPh_3)_3RhCl$	>50	>50	>50
Cisplatin	>50	12.07 ± 0.77	16.11 ± 0.89

hydroxyquinoline metal derivatives, **GUPT4**, containing–PPh_3 and —F ligands, was the most effective metal complex. Under the same conditions, the cytotoxic activity of **GUPT1**–**GUPT4** in CR-A549 cells followed the order: **GUPT4** > **GUPT3** > **GUPT2** > **GUPT1** > HGU1–HGU4 ligands ≈ $(PPh_3)_3RhCl$ ≈ cisplatin. Thus, **GUPT4** and **GUPT3** were chosen as the model rhodium(III)-8-hydroxyquinoline derivatives to elucidate the antineoplastic mechanism. Comparing complexes **GUPT1** and **GUPT2**, we found that the IC_{50} of the rhodium complex decreased in the presence of an electron-withdrawing substituent on the 8-hydroxyquinoline ligand. Comparing complexes **GUPT3** and **GUPT4**, we found that a greater electronegativity of the substituent on the 8-hydroxyquinoline ligand correlated with a lower IC_{50} of the rhodium complex. That is to say, the greater the electronegativity of the substituent on the ligand, the better the anticancer activity of the metal complex. This provides theoretical guidance for the synthesis of metal complexes with good anticancer activity.

2.3. Apoptosis

To study the model of cell apoptosis induced by **GUPT4** (5.11 μM) and **GUPT3** (8.74 μM), we assessed their pro-apoptotic effects on CR-A549 cells using flow cytometry (FCM) with Annexin V-APC and 7-AAD staining [43]. As depicted in Fig. 3, the treatment of CR-A549 cells with **GUPT4** (5.11 μM) and **GUPT3** (8.74 μM) resulted in apoptosis rates of 58.95 % and 37.60 %, respectively, indicating that both complexes induce apoptosis, with **GUPT4** being more effective (**GUPT4** > **GUPT3**). The results also indicated that the greater the electronegativity of the ligand substituent, the greater the ability of the complex to induce apoptosis. To be emphasized, the proportion of early and late apoptotic cells in the **GUPT4** treatment group was 52.93 % and 6.02 %, respectively, while 29.34 % in the early apoptotic and 8.26 % in the late apoptotic for **GUPT3**, indicating that **GUPT4** and **GUPT3** mainly induced cell death through early apoptosis. In addition, the proportion of necrotic cells in the **GUPT4** and **GUPT3** groups was only 6.45 % and 2.34 %, respectively. The cell necrosis rate were very low, indicating that the type of cell death in the **GUPT4** and **GUPT3** groups was apoptosis rather than necrosis.

2.4. Loss of the mitochondrial membrane potential ($\Delta\psi_{mp}$)

After stimulation, various coordination metal derivatives can decrease $\Delta\psi_{mp}$, an initiator of apoptosis [44,45]. To confirm this idea, the loss of $\Delta\psi_{mp}$ induced by **GUPT4** and **GUPT3** was assessed by the increase in green-to-red fluorescence ratio. As rhodium(III)-8-hydroxyquinoline derivatives can penetrate CR-A549 cells within 48 h (Fig. 4), the green fluorescence intensity for **GUPT4** (5.11 μM) and **GUPT3** (8.74 μM) reached approximately 65.50 % and 37.33 %, respectively, according to the FCM data. The results indicate that The greater the electronegativity of the substituent on the ligand, the greater the loss of the membrane potential $\Delta\psi_{mp}$ of the cell caused by the metal complex.

2.5. Analysis of reactive oxygen species (ROS) and [Ca^{2+}] levels

The destruction of $\Delta\psi_{mp}$ could also influence [Ca^{2+}] and intracellular ROS levels [46,47]. Thus, to evaluate the involvement of intracellular [Ca^{2+}] and ROS in CR-A549 cells, their levels following treatment with **GUPT4** (5.11 μM) and **GUPT3** (8.74 μM) were measured using Fluo-3AM and DCFH-DA assays, respectively. As illustrated in Figs. 5 and 6, compared with untreated cells, **GUPT4** and **GUPT3** significantly increased [Ca^{2+}] and ROS levels by 65.16 % and 66.92 % (**GUPT4**) and 37.42 % and 39.57 % (**GUPT3**), respectively. These results suggest that the elevation of [Ca^{2+}] and ROS levels contributed to the induction of apoptosis in CR-A549 cancer cells.

2.6. Evaluation of cellular respiration, ATP, and mitochondrial dysfunction

Mitochondrial dysfunction, characterized by the loss of $\Delta\psi_{mp}$, modulation of apoptosis-inducing factors/proteins, and reductions in mitochondrial state I/IV respiration and ATP production [48–50], is involved in apoptotic cell death. Western blot analysis was performed to study the apoptosis-inducing factors/proteins in apoptosis induced by **GUPT4** (5.11 μM) and **GUPT3** (8.74 μM) treatment. The ratios of cleaved-caspase-3/GAPDH, caspase-9/GAPDH, and cytochrome *c*/GAPDH increased in CR-A549 cells after treatment with **GUPT4** (5.11 μM) and **GUPT3** (8.74 μM), indicating that the apoptosis-inducing factors, cleaved-caspase-3, caspase-9, and cytochrome *c*, were released into the cytosol (Fig. 7). Additionally, we further tested whether **GUPT4** (5.11 μM) and **GUPT3** (8.74 μM) would inhibit state I/IV respiration and ATP production in CR-A549 cells using state I/IV respiration and ATP production kits [15e,48–50]. In **GUPT4**-and **GUPT3**-treated cells, a significant decrease in state I/IV respiration was observed (Tables 4 and S1–S3), and ATP synthase activity was inhibited. According to the results, both **GUPT4** and **GUPT3** can decrease state I/IV respiration and ATP production by targeting mitochondrial dysfunction.

2.7. Mitophagy determination

Mitophagy is a key mechanism for controlling mitochondrial damage

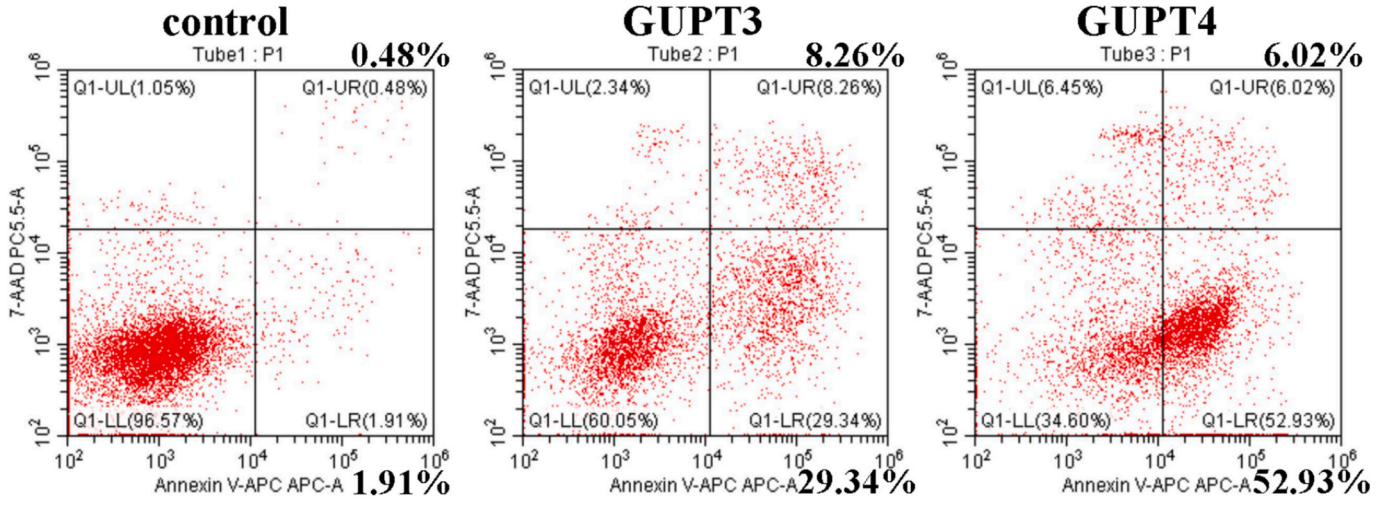

Fig. 3. Cell apoptosis induced by **GUPT4** (5.11 μM) and **GUPT3** (8.74 μM) after 48 h treatment in CR-A549 cells.

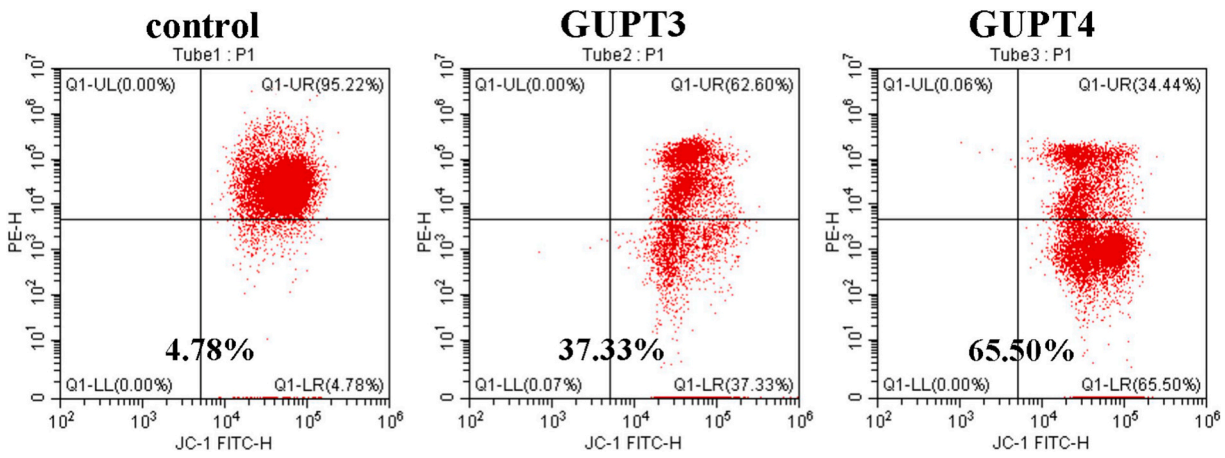

Fig. 4. Loss of $\Delta\psi_{mp}$ in CR-A549 cells induced by **GUPT4** (5.11 μM) and **GUPT3** (8.74 μM) after 48 h incubation.

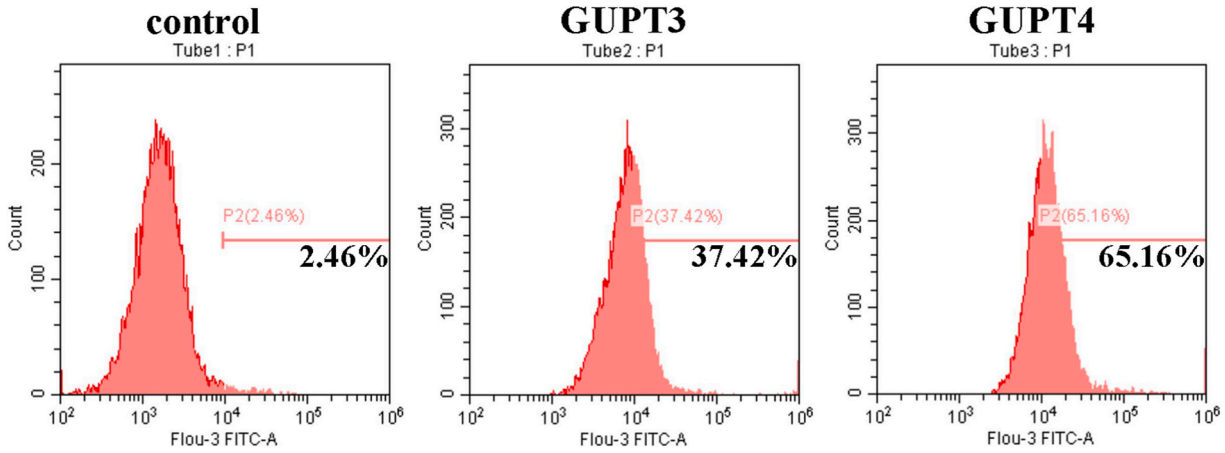

Fig. 5. Analysis of $[Ca^{2+}]$ in CR-A549 cells upon treatment with **GUPT4** (5.11 μM) and **GUPT3** (8.74 μM) for 48 h.

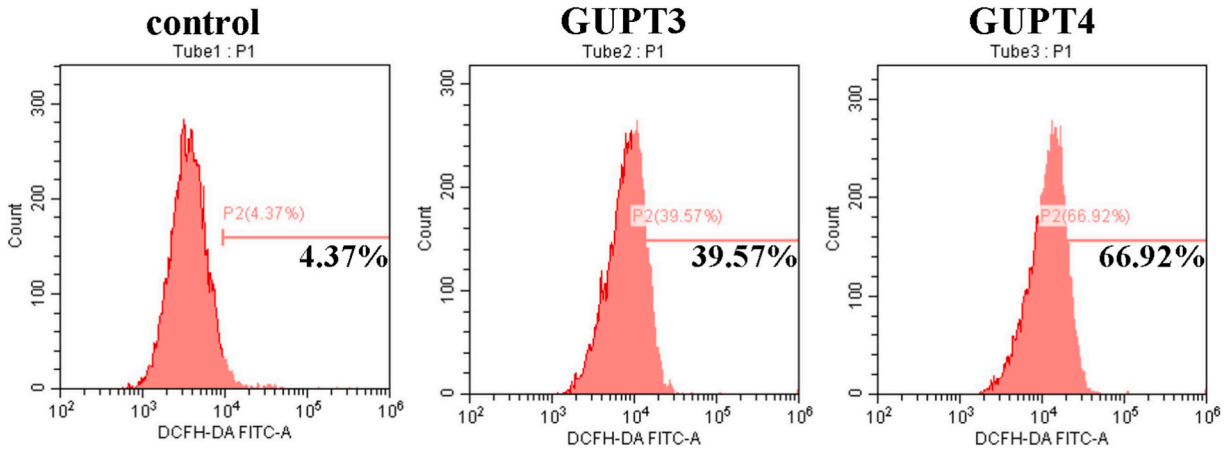

Fig. 6. Generation of ROS in CR-A549 cells were incubated with **GUPT4** (5.11 μM) and **GUPT3** (8.74 μM) for 48 h.

[15e,51–53]. Because rhodium(III)-8-hydroxyquinoline metal derivatives disrupt mitochondrial function, reduce state I/IV respiration, and decrease ATP production, they may induce mitophagy, which can subsequently trigger autophagy or cell apoptosis [15e,51–53]. To analyze the mitophagy process, the protein expressions of six known mitophagy markers, LC3B II/LC3B I, Beclin-1, P62, FUNDC1, PINK1, and Parkin, were evaluated in CR-A549 cells after treatment with **GUPT4** (5.11 μM) and **GUPT3** (8.74 μM) using Western blot analysis (Fig. 7). After 48 h of treatment, most key mitophagy-related markers were upregulated in **GUPT4**-and **GUPT3**-treated CR-A549 cells, while the levels of P62/GAPDH and FUNDC1/GAPDH were downregulated (Fig. 7), suggesting that mitochondrial mitophagy persisted for 48 h or longer. The results confirmed that **GUPT4** and **GUPT3** induced apoptosis in CR-A549 cells by triggering mitophagy and mitochondrial dysfunction, as well as by reducing state I/IV respiration and ATP production.

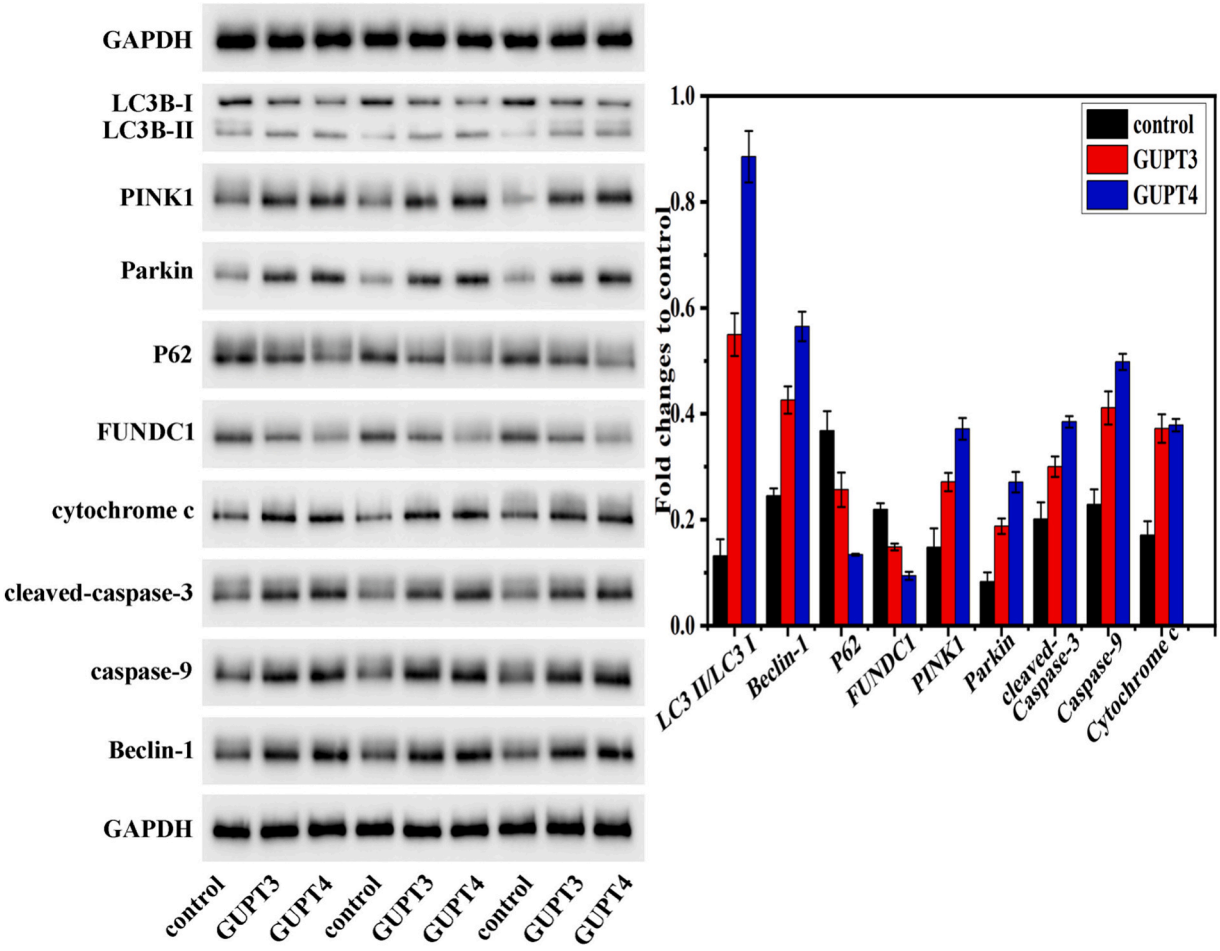

Fig. 7. Expression levels of mitophagy-and apoptosis-inducing factors/proteins in CR-A549 cells after GUPT4 (5.11 μM) and GUPT3 (8.74 μM) treatment for 48 h. GAPDH was used as the loading control for untreated (control) cells.

Table 4
Cellular state I/IV respiration and ATP production in CR-A549 cells treated with **GUPT4** (5.11 μM) and **GUPT3** (8.74 μM) for 48 h, as determined using state I/IV respiration and ATP production kits.

Groups	Complexes	Values
State I respiration	Control	95.59 ± 4.04 U/mg prot
	GUPT3	40.83 ± 2.15 U/mg prot
	GUPT4	26.29 ± 1.52 U/mg prot
State IV respiration	Control	83.69 ± 4.03 U/mg prot
	GUPT3	37.27 ± 1.25 U/mg prot
	GUPT4	24.64 ± 1.37 U/mg prot
ATP	Control	6.26 ± 0.34 μM
	GUPT3	2.68 ± 0.14 μM
	GUPT4	1.52 ± 0.13 μM

2.8. In vivo antiproliferative activity

To evaluate the in vivo therapeutic efficacy of **GUPT4** (5.0 mg/kg), an A549 tumor xenograft model was established, and the compound was administered intraperitoneally every 2 days for 21.0 days [48c,d]. **GUPT4** treatment resulted in significant tumor growth inhibition (~39.1 %) (Fig. 8), with no significant changes in body weight (Tables S4–S6), suggesting that **GUPT4** exhibits anticancer efficacy and safety in A549 tumor-bearing mice.

3. Conclusion

Four 5-halogenate-8-hydroxyquinoline rhodium(III)-triphenylphosphine complexes **GUPT1**–**GUPT4** have been presented. The anticancer activities of **GUPT1**–**GUPT4** against A549 and CR-A549 cells were investigated. **GUPT3** and **GUPT4** showed better anticancer activity than HGU1–HGU4, cisplatin, **GUPT1**, and **GUPT2**. Our investigation revealed that **GUPT3** and **GUPT4** induced oxidative stress (ROS) inside mitochondria, leading to mitophagy-mediated apoptosis in CR-A549 cells, with effectiveness in the following order: **GUPT3** < **GUPT4**. This mechanism highlights their potential as promising chemotherapeutic agents for apoptosis-resistant CR-A549 cell tumors. Moreover, the increased electronegativity of the ligand substituent correlates with the stronger anticancer activity of the rhodium complexes. In addition, **GUPT4** demonstrated significant anticancer activity (~39.1 % inhibition) and safety in A549 tumor-bearing mice. These findings provide theoretical guidance for the synthesis of rhodium complexes with high anticancer activity.

4. Experimental methods

4.1. Materials and instruments

4.1.1. Materials

The HGU1–HGU4 ligands and $(Ph_3P)_3$-RhCl were purchased from Energy Chemical and Aladdin. In addition, the Tris, gel loading buffer,

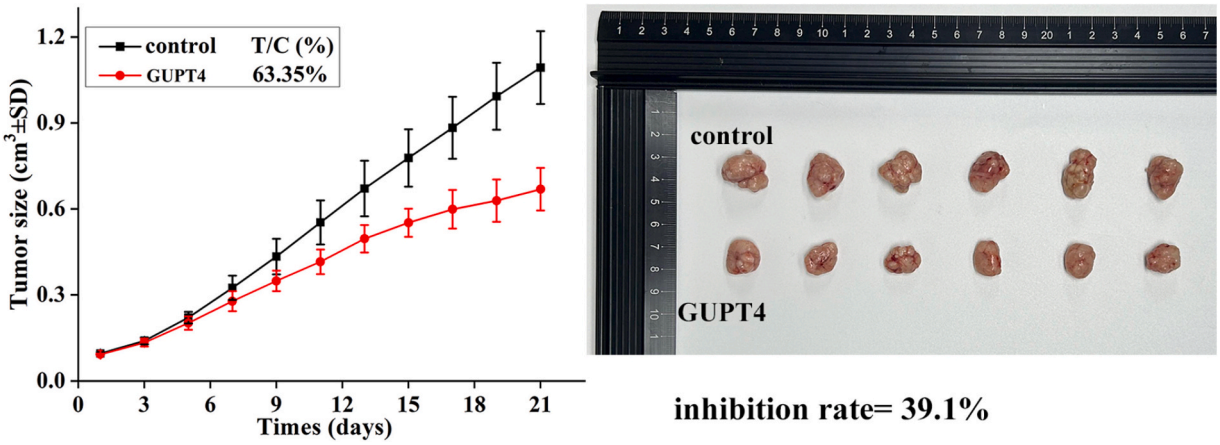

Fig. 8. Antiproliferative effect of **GUPT4** (5.0 mg/kg) on mice bearing A549 xenografts.

RNase A, Annexin V-APC, 7-AAD and propidium iodide (PI) were purchased from Sigma and BD. The antibody of cleaved-caspase-3, caspase-9, cytochrome *c*, LC3B II/LC3B I, Beclin-1, P62, FUNDC1, PINK1, Parkin, P62, GAPDH and FUNDC1 were purchased from Abcam. The Kits of ROS, Ca^{2+} and JC-1 were purchased from Jiangsu Kaige Biotechnology Co., Ltd. The CR-A549, A549 and HEK293 cell lines were obtained from the Shanghai Institute for Biological Science (China). The ATP assay kit (United Kingdom, Abcam ab113849) and state I/IV respiration assay kits (Beijing Solarbio, China, BC0515 and BC0945) were obtained from Abcam and Beijing Solarbio Science & Technology Co., Ltd.

4.1.2. Instruments

Elemental analyses (C, H and N) were carried out on a PerkinElmer series II CHNS/O 2400 elemental analyzer. The ^{1}H NMR spectra was recorded on a Bruker AV-400 NMR spectrometer. ESI-MS spectra was performed on Thermofisher Scientific Exactive LC-MS spectrometer (Thermal Elctronic, USA). Apoptosis assay, ROS, Ca^{2+} and JC-1 analysis were recorded on Flow cytometer (BECKMAN COULTER CytoFLEX). The absorbance of CCK-8 assay was determined by measuring the optical density at 450 nm using a multifunctional enzyme marker (n = 5, Switzerland, TECAN SPARK).

4.2. Synthesis of GUPT1

The ligand HGU1 (0.05 mmol, 7.3 mg) and $(Ph_3P)_3RhCl$ (0.05 mmol, 46.3 mg) were dissolved in MeOH (0.6 mL), CH_2Cl_2 (0.1 mL) and triethylamine (0.1 mL), and then, the mixture in the HTRT (15.0 mL) was sealed and placed in an oven at 65 °C for 1.0 day and at 80 °C for 3.0 days (Scheme 1). After 1.0 day, the reddish-brown lumpy crystals of **GUPT1** were obtained. Yield: 60.5 %. Elemental analysis: calcd (%) for $RhC_{45}H_{36}OCl_2NP_2$: C 64.15, H 4.31, N 1.66; found: C 64.16, H 4.35, N 1.65. ^{1}H NMR (400 MHz, DMSO-d_6, Fig. S3): δ 7.66–7.59 (m, 8H), 7.55 (m, 6H), 7.44–7.37 (m, 6H), 7.36–7.31 (m, 3H), 7.24 (m, 7H), 7.19–7.13 (m, 2H), 6.97 (m, 4H).

4.3. Synthesis of GUPT2

Replacing HGU1 (0.05 mmol, 7.3 mg) with HGU2 (0.05 mmol, 11.2 mg) with the procedure for **GUPT1** gave rise to **GUPT2**. Yield: 54.2 %. Elemental analysis: calcd (%) for $RhC_{45}H_{35}OBrCl_2NP_2$: C 58.66, H 3.83, N 1.52; found: C 58.63, H 3.81, N 1.55. ^{1}H NMR (400 MHz, DMSO-d_6, Fig. S4): δ 7.65–7.59 (m, 8H), 7.58–7.52 (m, 6H), 7.42–7.38 (m, 5H), 7.36–7.32 (m, 3H), 7.30–7.23 (m, 6H), 7.20–7.14 (m, 3H), 6.99–6.94 (dd, J = 8.5, 3.0 Hz, 4H). ESI-MS (positive ion mode, Fig. S1): m/z: 713.85 $[M + 4(DMSO) + 3(H_2O) + H]^+$.

4.4. Synthesis of GUPT3

Replacing HGU1 (0.05 mmol, 7.3 mg) with HGU3 (0.10 mmol, 18.0 mg) with the procedure for **GUPT1** gave rise to **GUPT3**. Yield: 40.8 %. Elemental analysis: calcd (%) for $RhC_{36}H_{25}O_2Cl_3N_2P$: C 57.06, H 3.33, N 3.70; found: C 57.07, H 3.35, N 3.73. ESI-MS (positive ion mode, Fig. S2): m/z: 1126.56 $[M-(Ph_3P) + 3(H_2O) + H]^+$.

4.5. Synthesis of GUPT4

Replacing HGU1 (0.05 mmol, 7.3 mg) with HGU4 (0.10 mmol, 16.3 mg) with the procedure for **GUPT1** gave rise to **GUPT4**. Yield: 56.7 %. Elemental analysis: calcd (%) for $RhC_{36}H_{25}O_2ClF_2N_2P$: C 59.65, H 3.48, N 3.86; found: C 59.66, H 3.50, N 3.85. ^{1}H NMR (400 MHz, DMSO-d_6, Fig. S5): δ 7.65–7.59 (m, 7H), 7.58–7.54 (m, 4H), 7.42–7.35 (m, 5H), 7.30–7.23 (m, 3H), 7.18 (m, 2H), 7.01–6.96 (m, 4H).

4.6. Biological experiments

The A549 and CR-A549 cells were cultured in six-well plates (SWP) at a density of 5.0×10^5 cells per well for 24 h. After incubation with **GUPT4** (5.11 μM) and **GUPT3** (8.74 μM) for 48 h, the CR-A549 cells were harvested from SWP, and Annexin V-APC (5.0 μL)/7-AAD (5.0 μL) double dyeing (for apoptosis test), Fluo-3AM (1.0 μM) fluorescence probe (for $[Ca^{2+}]$), DCFH-DA (10.0 μM) fluorochrome (for ROS), and JC-1 (1.0 μL) staining (for $\Delta\psi_{mp}$) were added to the CR-A549 cells and incubated for 30.0 min at 37.0 °C. And then the fluorescence intensity for SWP sample was measured by FCM analysis. In addition, The release of the state I/IV respiration and ATP in the **GUPT4** (5.11 μM)-and **GUPT3** (8.74 μM)-treated cells were detected with state I/IV respiration and ATP assay system bioluminescence detection kit.

4.7. The other methods

The other methods of **GUPT1**–**GUPT4** were similar to those illustrated in previous work [15e,48,54]. In addition, the detailed antiproliferative activity of **GUPT4** (5.0 mg/kg) in vivo as regards A549 cells can be found in the ESI.

CRediT authorship contribution statement

Zhen-Feng Wang: Methodology, Formal analysis, Data curation. **Xiao-Qiong Huang:** Data curation. **Run-Chun Wu:** Formal analysis. **Shu-Hua Zhang:** Writing – review & editing, Writing – original draft, Supervision, Project administration. **Guangzhao Li:** Writing – review & editing, Writing – original draft, Project administration.

Declaration of competing interest

We declare that have no financial and personal relationships with other people or organizations that can inappropriately influence our work, there is no professional or other personal interest of any nature of kind in any product, service and/or company that could be constructed as influencing the position pressented in, or the review of, the manscript entitled.

Acknowledgments

This work was supported by the National Natural Science Foundation of China (No. 21861014), the Talent introduction program of Guangdong Institute of Petrochemical Technology (Nos. 2020RC033, 2020RC002, 2020RC035) and the China University Students Innovative Project (Nos. 202410606027 and 202410606025).

Appendix A. Supplementary data

Supplementary data to this article can be found online at https://doi.org/10.1016/j.bioorg.2025.108789.

Data availability

Data will be made available on request.

References

[1] (a) D.-L. Ma, M. Wang, Z. Mao, C. Yang, C.-T. Ng, C.-H. Leung, Dalton Trans. 45 (2016) 2762–2771;
(b) B. Zhang, Z. Xu, W. Zhou, Z. Liu, J. Zhao, S. Gou, Chem. Sci. 12 (2021) 11810–11820;
(c) F. Wei, S. Kuang, T.W. Rees, X. Liao, J. Liu, D. Luo, J. Wang, X. Zhang, L. Ji, H. Chao, Biomaterials 276 (2021) 121064;
(d) M. Sohrabi, M.B. Torbati, M. Lutz, S. Meghdadi, H. Farrokhpour, A. Amiri, M. Amirnasr, J. Photochem. Photobiol. A: Chem. 423 (2022) 113573;
(e) Y.-B. Peng, W. He, Q. Niu, C. Tao, X.-L. Zhong, C.-P. Tan, P. Zhao, Dalton Trans. 50 (2021) 9068–9075.

[2] (a) J.-J. Zhang, J.K. Muenzner, M.A. Abu el Maaty, B. Karge, R. Schobert, S. Wölfl, I. Ott, Dalton Trans. 45 (2016) 13161–13168;
(b) P. Chellan, V.M. Avery, S. Duffy, K.M. Land, C.C. Tam, J.H. Kim, L.W. Cheng, I. Romero-Canelón, P.J. Sadler, J. Inorg. Biochem. 219 (2021) 111408.

[3] (a) Z.-F. Wang, X.-L. Nai, Y. Xu, F.-H. Pan, F.-S. Tang, Q.-P. Qin, L. Yang, S.-H. Zhang, Dalton Trans. 51 (2022) 12866–12875;
(b) X. He, J. Chen, M. Kandawa-Shultz, G. Shao, Y. Wang, Dalton Trans. 52 (2023) 4728–4736;
(c) U. Das, B. Kar, S. Pete, P. Paira, Dalton Trans. 50 (2021) 11259–11290.

[4] (a) N. Katsaros, A. Anagnostopoulou, Crit. Rev. Oncol. Hematol. 42 (2002) 297–308;
(b) T.S. Prathima, B. Choudhury, M.G. Ahmad, K. Chanda, M.M. Balamurali, Coordin. Chem. Rev. 490 (2023) 215231;
(c) D. Loreto, A. Merlino, Coordin. Chem. Rev. 442 (2021) 213999;
(d) P. Štarha, Coordin. Chem. Rev. 431 (2021) 213690.

[5] (a) K.K.H. Tong, M. Riisom, E. Leung, M. Hanif, T. Söhnel, S.M.F. Jamieson, C. G. Hartinger, Inorg. Chem. 61 (2022) 17226–17241;
(b) A. Sink, S. Banerjee, J.A. Wolny, C. Imberti, E.C. Lant, M. Walker, V. Schünemann, P.J. Sadler, Dalton Trans. 51 (2022) 16070–16081.

[6] Y. Zheng, X.-X. Chen, D.-Y. Zhang, W.-J. Wang, K. Peng, Z.-Y. Li, Z.-W. Mao, C.-P. Tan, Chem. Sci. 14 (2023) 6890–6903.

[7] Dianna Truong, Matthew P. Sullivan, Kelvin K.H. Tong, Tasha R. Steel, Andre Prause, James H. Lovett, J.W. Andersen, S.M.F. Jamieson, H.H. Harris, I. Ott, C.M. Weekley, K. Hummitzsch, T. Sohnel, M. Hanif, N. Metzler-Nolte, D. C. Goldstone, C.G. Hartinger, Inorg. Chem. 59 (2020) 3281–3289.

[8] R.M. Lord, M. Zegke, A.M. Basri, C.M. Pask, P.C. McGowan, Inorg. Chem. 60 (2021) 2076–2086.

[9] A. Nahaei, Z. Mandegani, S. Chamyani, M. Fereidoonnezhad, H.R. Shahsavari, N. Y. Kuznetsov, S.M. Nabavizadeh, Inorg. Chem. 61 (2022) 2039–2056.

[10] (a) A. Petrović, M. Živanović, R. Puchta, D. Ćoćić, A. Scheurer, N. Milivojevic, J. Bogojeski, Dalton Trans. 49 (2020) 9070–9085;
(b) S. Banerjee, J.J. Soldevila-Barreda, J.A. Wolny, C.A. Wootton, A. Habtemariam, I. Romero-Canelon, F. Chen, G.J. Clarkson, I. Prokes, L. Song, P. B. O'Connor, V. Schxunemann, P.J. Sadler, Chem. Sci. 9 (2018) 3177–3185;
(c) W.-Y. Zhang, H.E. Bridgewater, S. Banerjee, J.J. Soldevila-Barreda, G. J. Clarkson, H. Shi, C. Imberti, P.J. Sadler, Eur. J. Inorg. Chem. (2020) 1052–1060.

[11] M. Hanif, J. Arshad, J.W. Astin, Z. Rana, A. Zafar, S. Movassaghi, E. Leung, K. Patel, T. Sçhnel, J. Reynisson, V. Sarojini, R.J. Rosengren, S.M.F. Jamieson, C. G. Hartinger, Angew. Chem. Int. Ed. 59 (2020) 14609–14614.

[12] M. Fandzloch, A.W. Augustyniak, L. Dobrzańska, T. Jędrzejewski, J. Sitkowski, M. Wypij, P. Golińska, J. Inorg. Biochem. 210 (2020) 111072.

[13] (a) S. Saha, R. Kushwaha, A. Mandal, N. Singh, S. Banerjee, Coord. Chem. Rev. 525 (2025) 216306;
(b) Y.-Q. Gu, M.-X. Ma, Q.-Y. Yang, K. Yang, H.-Q. Li, M.-Q. Hu, H. Liang, Z.-F. Chen, Bioorg. Chem. 141 (2023) 106838.

[14] L. Guo, X. Hu, Y. Yang, W. An, J. Gao, Q. Liu, Z. Liu, Bioorg. Chem. 116 (2021) 105311.

[15] (a) R. Gupta, V. Luxami, K. Paul, Bioorg. Chem. 108 (2021) 104633;
(b) V. Oliveri, V. Lanza, D. Milardi, M. Viale, I. Maric, C. Sgarlata, G. Vecchio, Metallomics 9 (2017) 1439–1446;
(c) T. Meng, Q.-P. Qin, Z.-L. Chen, H.-H. Zou, K. Wang, F.-P. Liang, Eur. J. Med. Chem. 169 (2019) 103–110;
(d) V.F.S. Pape, N.V. May, G.T. Gál, I. Szatmári, F. Szeri, F. Fülöp, G. Szakács, É. A. Enyedy, Dalton Trans. 47 (2018) 17032–17045;
(e) Z.-F. Wang, X.-Q. Huang, R.-C. Wu, Y. Xiao, S.-H. Zhang, J. Inorg. Biochem. 248 (2023) 112361.

[16] (a) Q.-P. Qin, Z.-F. Wang, M.-X. Tan, X.-L. Huang, H.-H. Zou, B.-Q. Zou, B.-B. Shi, S.-H. Zhang, Metallomics 11 (2019) 1005–1015;
(b) Y. Yang, Z. Zhou, Z.-Z. Wei, Q.-P. Qin, L. Yang, H. Liang, Dalton Trans. 50 (2021) 5828–5834;
(c) R. Wang, B.-Q. Zou, Q.-P. Qin, Z.-F. Wang, M.-X. Tan, H. Liang, Transit. Met. Chem. 45 (2020) 477–483;
(d) F. Bisceglie, A. Musiari, S. Pinelli, R. Alinovi, I. Menozzi, E. Polverini, P. Tarasconi, M. Tavone, G. Pelosi, J. Inorg. Biochem. 152 (2015) 10–19.

[17] (a) Z.-F. Wang, Q.-C. Wei, J.-X. Li, Z. Zhou, S.-H. Zhang, Dalton Trans. 51 (2022) 7154–7163;
(b) A. Kotian, V. Kamat, K. Naik, D.G. Kokare, K. Kumara, K.L. Neratur, V. Kumbar, K. Bhat, V.K. Revankar, Bioorg. Chem. 112 (2021) 104962;
(c) I. Potočňák, P. Vranec, V. Farkasová, D. Sabolová, M. Vataščinová, J. Kudláčová, I.D. Radojević, L.R. Čomić, B.S. Markovic, V. Volarevic, N. Arsenijevic, S.R. Trifunović, J. Inorg. Biochem. 154 (2016) 67–77;
(d) N. Gligorijević, T. Todorović, S. Radulović, D. Sladić, N. Filipović, D. Gođevac, D. Jeremić, K. Anđelković, Eur. J. Med. Chem. 44 (2009) 1623–1629.

[18] (a) Y.-F. Wang, J.-X. Tang, Z.-Y. Mo, J. Li, F.-P. Liang, H.-H. Zou, Dalton Trans. 51 (2022) 8840–8847;
(b) J.Y.-C. Chang, G.-L. Lu, R.J. Stevenson, P.J. Brothers, G.R. Clark, K.J. Botting, D.M. Ferry, M. Tercel, W.R. Wilson, W.A. Denny, D.C. Ware, Inorg. Chem. 52 (2013) 7688–7698;
(c) T. Meng, Q.-P. Qin, H.-H. Zou, K. Wang, F.-P. Liang, ACS Med. Chem. Lett. 10 (2019) 1603–1608.

[19] (a) Q. Tang, W.-X. Ni, C.-F. Leung, W.-L. Man, K.K.-K. Lau, Y. Liang, Y.-W. Lam, W.-Y. Wong, S.-M. Peng, G.-J. Liu, T.-C. Lau, Chem. Commun. 49 (2013) 9980–9982;
(b) L.-Q. Du, C.-J. Zeng, D.-Y. Mo, Q.-P. Qin, M.-X. Tan, H. Liang, J. Inorg. Biochem. 251 (2024) 112443;
(c) L. Yang, J. Zhang, C. Wang, X. Qin, Q. Yu, Y. Zhou, J. Liu, Metallomics 6 (2014) 518–531;
(d) X. He, J. Chen, M. Kandawa-Shultz, G. Shao, Y. Wang, Dalton Trans. 52 (2023) 4728–4736.

[20] (a) N. Khaorapapong, P. Pimchan, M. Ogawa, Dalton Trans. 40 (2011) 5964–5970;
(b) G.F. Condike, A.E. Martell, J. Inorg. Nucl. Chem. 31 (1969) 2455–2466;
(c) S. Sangeetha, T. Ajaykamal, M. Murali, New J. Chem. 45 (2021) 7578–7593;
(d) G.J. Kharadi, J.R. Patel, B.Z. Dholakiya, Appl. Orgamomet. Chem. 24 (2010) 821–827;
(e) Q.-P. Qin, Z.-F. Chen, J.-L. Qin, X.-J. He, Y.-L. Li, Y.-C. Liu, K.-B. Huang, H. Liang, Eur. J. Med. Chem. 92 (2015) 302–313;
(f) Y. Yang, L.-Q. Du, Y. Huang, C.-J. Liang, Q.-P. Qin, H. Liang, J. Inorg. Biochem. 241 (2023) 112152.

[21] (a) M. Zhang, L. Li, S. Li, Z. Liu, N. Zhang, B. Sun, Z. Wang, D. Jia, M. Liu, Q. Wang, J. Med. Chem. 66 (2023) 3393–3410;
(b) Q.-P. Qin, S.-L. Wang, M.-X. Tan, Y.-C. Liu, T. Meng, B.-Q. Zou, H. Liang, Eur. J. Med. Chem. 161 (2019) 334–342;
(c) C.M. Santos, S. Cabrera, C. Rios-Luci, J.M. Padron, I.L. Solera, A.G. Quiroga, M. A. Medrano, C. Navarro-Ranninger, J. Aleman, Dalton Trans. 42 (2013) 13343–13348;
(d) T.-M. Shao, Z.-Z. Wei, X.-L. Luo, Q.-P. Qin, M.-X. Tan, J.-J. Zeng, C.-J. Liang, H. Liang, New J. Chem. 44 (2020) 19885–19890.

[22] (a) K.L. Summers, M.J. Pushie, G.J. Sopasis, A.K. James, N.V. Dolgova, D. Sokaras, T. Kroll, H.H. Harris, I.J. Pickering, G.N. George, Inorg. Chem. 59 (2020) 13858–13874;
(b) B. Deka, T. Sarkar, S. Banerjee, A. Kumar, S. Mukherjee, S. Deka, K.K. Saikia, A. Hussain, Dalton Trans. 46 (2017) 396–409;
(c) S. Sangeetha, T. Ajaykamal, M. Murali, New J. Chem. 45 (2021) 7578–7593;
(d) V. Oliveri, M. Viale, G. Caron, C. Aiello, R. Gangemi, G. Vecchio, Dalton Trans. 42 (2013) 2023–2034.

[23] (a) H. Seo, M.K. Jackl, M. Kalaj, S.M. Cohen, Inorg. Chem. 61 (2022) 7631–7641;
(b) X. Jia, F.-F. Yang, J. Li, J.-Y. Liu, J.-P. Xue, J. Med. Chem. 56 (2013) 5797–5805;
(c) Y.-C. Liu, J.-H. Wei, Z.-F. Chen, M. Liu, Y.-Q. Gu, K.-B. Huang, Z.-Q. Li, H. Liang, Eur. J. Med. Chem. 69 (2013) 554–563;
(d) L.-Q. Du, T.-Y. Zhang, X.-M. Huang, Y. Xu, M.-X. Tan, Y. Huang, Y. Chen, Q.-P. Qin, Dalton Trans. 52 (2023) 4737–4751.

[24] (a) S. Tardito, A. Barilli, I. Bassanetti, M. Tegoni, O. Bussolati, R. Franchi-Gazzola, C. Mucchino, L. Marchio, J. Med. Chem. 55 (2012) 10448–10459;

(b) L.W. Njenga, S.N. Mbugua, R.A. Odhiambo, M.O. Onani, Dalton Trans. 52 (2023) 5823–5847;
(c) D. Rogolino, A. Cavazzoni, A. Gatti, M. Tegoni, G. Pelosi, V. Verdolino, C. Fumarola, D. Cretella, P.G. Petronini, M. Carcelli, Eur. J. Med. Chem. 128 (2017) 140–153.
[25] (a) T. Meng, Q.-P. Qin, Z.-L. Chen, H.-H. Zou, K. Wang, F.-P. Liang, Eur. J. Med. Chem. 192 (2020) 112192;
(b) L.-Q. Qin, B.-Q. Zou, Q.-P. Qin, Z.-F. Wang, L. Yang, M.-X. Tan, C.-J. Liang, H. Liang, New J. Chem. 44 (2020) 7832–7837;
(c) Y. Yang, C.-M. Wang, F.-H. Pan, Q.-P. Qin, Q.-J. Xie, Q. Chen, H. Liang, Dalton Trans. 50 (2021) 16273–16280.
[26] R. Kumar, A. Thakur, D. Sachin, A.K. Chandra, P.K. Dhiman, U. Sharma Verma, Coordin, Chem. Rev. 499 (2024) 215453.
[27] H.-R. Zhang, Y.-C. Liu, Z.-F. Chen, T. Meng, B.-Q. Zou, Y.-N. Liu, H. Liang, New J. Chem. 40 (2016) 6005–6014.
[28] O. Dömötör, V.F.S. Pape, N.V. May, G. Szakácsc, É.A. Enyedy, Dalton Trans. 46 (2017) 4382–4396.
[29] (a) J.P. Mészáros, J.M. Poljarević, I. Szatmári, O. Csuvik, F. Fülöp, N. Szoboszlai, G. Spengler, É.A. Enyedy, Dalton Trans. 49 (2020) 7977–7992;
(b) O. Dömötör, T. Pivarcsik, J.P. Mészáros, I. Szatmári, F. Fülöp, É.A. Enyedy, Dalton Trans. 50 (2021) 11918–11930;
(c) T. Pivarcsik, O. Dömötör, J.P. Mészáros, N.V. May, G. Spengler, O. Csuvik, I. Szatmári, É.A. Enyedy, Int. J. Mol. Sci. 22 (2021) 11281.
[30] Y.-L. Zhang, Q.-P. Qin, Q.-Q. Cao, H.-H. Han, Z.-L. Liu, Y.-C. Liu, H. Liang, Z.-F. Chen, Med. Chem. Commun. 8 (2017) 184–190.
[31] Z. Zhu, Z. Wang, C. Zhang, Y. Wang, H. Zhang, Z. Gan, Z. Guo, X. Wang, Mitochondrion-targeted platinum complexes suppressing lung cancer through multiple pathways involving energy metabolism, Chem. Sci. 10 (2019) 3089–3095.
[32] Z. Liu, H. Fu, H. Dong, K. Lai, Z. Yang, C. Fan, Y. Luo, W. Qin, L. Guo, Triphenylphosphine-modified IridiumIII, RhodiumIII, and RutheniumII complexes to achieve enhanced anticancer selectivity by targeting mitochondria, Inorg. Chem. 63 (2024) 24736–24753.
[33] S. Li, J. Zhao, Y. Guo, Y. Mei, B. Yuan, N. Gan, J. Zhang, J. Hu, H. Hou, Influence of the introduction of a Triphenylphosphine group on the anticancer activity of a copper complex, J. Inorg. Biochem. 210 (2020) 111102.
[34] M.R. Newby, Experimental and Computational Studies of Unusual P-Donor Ligands and their Coordination Chemistry, University of Bristol, 2022. http://research-information.bristol.ac.uk.
[35] M. Shabbir, Z. Akhter, A.R. Ashraf, H. Ismail, A. Habib, B. Mirza, Nickel (II) and palladium (II) triphenylphosphine complexes incorporating tridentate Schiff base ligands: synthesis, characterization and biocidal activities, J. Mol. Struct. 1149 (2017) 720–726.
[36] (a) P.G. Nandi, P.K. Jadi, K. Das, S.J. Prathapa, B.B. Mandal, A. Kumar, Inorg. Chem. 60 (2021) 7422–7432;
(b) J. Cervinka, A. Gobbo, L. Biancalana, L. Markova, V. Novohradsky, M. Guelfi, S. Zacchini, J. Kasparkova, V. Brabec, F. Marchetti, J. Med. Chem. 65 (2022) 10567–10587;
(c) C. Scolaro, A.B. Chaplin, C.G. Hartinger, A. Bergamo, M. Cocchietto, B. K. Keppler, G. Sava, P.J. Dyson, Dalton Trans. (2007) 5065–5072.
[37] (a) A. Gobbo, S.A.P. Pereira, L. Biancalana, S. Zacchini, M.L.M.F.S. Saraiva, P. J. Dyson, F. Marchetti, Dalton Trans. 51 (2022) 17050–17063;
(b) G. Sahu, S.A. Patra, S. Lima, S. Das, H. Gorls, W. Plass, R. Dinda, Chem. Eur. J. 29 (2023) e202202694;
(c) L.C.-C. Lee, K.K.-W. Lo, J. Am. Chem. Soc. 144 (2022) 14420–14440.
[38] (a) T. Meng, S.-F. Tang, Q.-P. Qin, Y.-L. Liang, C.-X. Wu, C.-Y. Wang, H.-T. Yan, J.-X. Dong, Y.-C. Liu, Med. Chem. Commun. 7 (2016) 1802–1811;
(b) C.M. Santos, S. Cabrera, C. Rios-Luci, J.M. Padron, I.L. Solera, A.G. Quiroga, M.A. Medrano, C. Navarro-Ranninger, J. Aleman, Dalton Trans. 42 (2013) 13343–13348.
[39] (a) A. Groué, J.-P. Tranchier, M.N. Rager, G. Gontard, R. Métivier, O. Buriez, A. Khatyr, M. Knorr, H. Amouri, Inorg. Chem. 61 (2022) 4909–4918;
(b) Y.-Q. Gu, K. Yang, Q.-Y. Yang, H.-Q. Li, M.-Q. Hu, M.-X. Ma, N.-F. Chen, Y.-H. Liu, H. Liang, Z.-F. Chen, J. Med. Chem. 66 (2023) 9592–9606;
(c) L. Guo, P. Li, J. Li, Y. Gong, X. Li, Y. Liu, K. Yu, Z. Liu, Inorg. Chem. 62 (2023) 15118–15137.
[40] (a) F. Hackenberg, L. Oehninger, H. Alborzinia, S. Can, I. Kitanovic, Y. Geldmacher, M. Kokoschka, S. Wölfl, I. Ott, W.S. Sheldrick, J. Inorg. Biochem. 105 (2011) 991–999;
(b) C.G.L. Nongpiur, A.K. Verma, R.K. Singh, M.M. Ghate, K.M. Poluri, W. Kaminsky, M.R. Kollipara, J. Inorg. Biochem. 238 (2023) 112059.
[41] M. Manikandan, S. Gadre, S. Chhatar, G. Chakraborty, N. Ahmed, C. Patra, M. Patra, J. Med. Chem. 65 (2022) 16353–16371.
[42] (a) D. Romani, F. Marchetti, C. Di Nicola, M. Cuccioloni, C. Gong, A. Maria Eleuteri, A. Galindo, F. Fadaei-Tirani, M. Nabissi, R. Pettinari, J. Med. Chem. 66 (2023) 3212–3225;
(b) X.-D. Song, X. Kong, S.-F. He, J.-X. Chen, J. Sun, B.-B. Chen, J.-W. Zhao, Z.-W. Mao, Eur. J. Med. Chem. 138 (2017) 246–254.
[43] (a) Y. Yang, Y. Gao, Y. Sun, J. Zhao, S. Gou, J. Med. Chem. 66 (2023) 13731–13745;
(b) Q.-P. Qin, Z.-F. Wang, X.-L. Huang, M.-X. Tan, Z.-H. Luo, S.-L. Wang, B.-Q. Zou, H. Liang, Dalton Trans. 48 (2019) 15247–15254;
(c) T. Meng, Q.-P. Qin, Z.-R. Wang, L.-T. Peng, H.-H. Zou, Z.-Y. Gan, M.-X. Tan, K. Wang, F.-P. Liang, J. Inorg. Biochem. 189 (2018) 143–150;
(d) Q.-P. Qin, Z.-F. Wang, X.-L. Huang, M.-X. Tan, B.-Q. Zou, H. Liang, Eur. J. Med. Chem. 184 (2019) 111751.
[44] (a) W. Wang, P. Wang, X. Liao, B. Yang, C. Gao, J. Yang, J. Med. Chem. 66 (2023) 13103–13115;
(b) M. Negi, T. Dixit, V. Venkatesh, Inorg. Chem. 62 (2023) 20080–20095.
[45] L. Wang, X. Liu, Y. Wu, X. He, X. Guo, W. Gao, L. Tan, X.-A. Yuan, J. Liu, Z. Liu, Inorg. Chem. 62 (2023) 3395–3408.
[46] (a) L. Cai, Y. Wang, H. Chen, Y. Tan, T. Yang, S. Zhang, Z. Guo, X. Wang, J. Med. Chem. 66 (2023) 11351–11364;
(b) A. Hernández-García, L. Marková, M.D. Santana, J. Pracharová, D. Bautista, H. Kostrhunová, V. Novohradsky, V. Brabec, J. Ruiz, J. Kaspárková, Inorg. Chem. 62 (2023) 6474–6487.
[47] (a) A. Upadhyay, P. Kundu, V. Ramu, P. Kondaiah, A.R. Chakravarty, Inorg. Chem. 61 (2022) 1335–1348;
(b) L.-S. Liao, Y. Chen, C. Hou, Y.-H. Liu, G.-F. Su, H. Liang, Z.-F. Chen, J. Med. Chem. 66 (2023) 10497–10509;
(c) Y.-Q. Gu, Y.-J. Zhong, M.-Q. Hu, H.-Q. Li, K. Yang, Q. Dong, H. Liang, Z.-F. Chen, Dalton Trans. 51 (2022) 1968–1978.
[48] (a) Z. Yang, M. Bian, L. Lv, X. Chang, Z. Wen, F. Li, Y. Lu, W. Liu, J. Med. Chem. 66 (2023) 3934–3952;
(b) A.S. Arojojoye, C. Olelewe, S. Gukathasan, J.H. Kim, H. Vekaria, S. Parkin, P. G. Sullivan, S.G. Awuah, J. Med. Chem. 66 (2023) 7868–7879;
(c) Z.-F. Wang, X.-F. Zhou, Q.-C. Wei, Q.-P. Qin, J.-X. Li, M.-X. Tan, S.-H. Zhang, Eur. J. Med. Chem. 238 (2022) 114418;
(d) S.-H. Zhang, Z.-F. Wang, H. Tan, Eur. J. Med. Chem. 243 (2022) 114736.
[49] (a) R.J. Mitchell, A.S. Gowda, A.G. Olivelli, A.J. Huckaba, S. Parkin, J.M. Unrine, V. Oza, J.S. Blackburn, F. Ladipo, D.K. Heidary, E.C. Glazer, Inorg. Chem. 62 (2023) 10940–10954;
(b) X. Bai, A. Ali, Z. Lv, N. Wang, X. Zhao, H. Hao, Y. Zhang, F.-U. Rahman, Eur. J. Med. Chem. 224 (2021) 113689;
(c) J. Liu, Y. Chen, G. Li, P. Zhang, C. Jin, L. Zeng, L.-N. Ji, H. Chao, Biomaterials 56 (2015) 140–153.
[50] (a) L. Chen, J. Wang, X. Cai, S. Chen, J. Zhang, B. Li, W. Chen, X. Guo, H. Luo, J. Chen, Bioorg. Chem. 119 (2022) 105516;
(b) N. Roy, U. Sen, Y. Madaan, V. Muthukumar, S. Varddhan, S.K. Sahoo, D. Panda, B. Bose, P. Paira, Inorg. Chem. 59 (2020) 17689–17711;
(c) M. Shao, M. Yao, X. Liu, C. Gao, W. Liu, J. Guo, J. Zong, X. Sun, Z. Liu, Inorg. Chem. 60 (2021) 17063–17073.
[51] (a) Z. Zhou, L.-Q. Du, X.-M. Huang, L.-G. Zhu, Q.-C. Wei, Q.-P. Qin, H. Bian, Eur. J. Med. Chem. 243 (2022) 114743;
(b) W. Ma, S. Zhang, Z. Tian, Z. Xu, Y. Zhang, X. Xia, X. Chen, Z. Liu, Eur. J. Med. Chem. 181 (2019) 111599.
[52] (a) C.-P. Tan, Y.-M. Zhong, L.-N. Ji, Z.-W. Mao, Chem. Sci. 12 (2021) 2357–2367;
(b) R.D. Mule, A. Kumar, S.P. Sancheti, B. Senthilkumar, H. Kumar, N.T. Patil, Chem. Sci. 13 (2022) 10779–10785;
(c) Z. Liu, G. Qin, J. Yang, W. Wang, W. Zhang, B. Lu, J. Ren, X. Qu, Chem. Sci. 14 (2023) 11192–11202.
[53] (a) J.-J. Zhang, Q.-J. Xu, C. Schmidt, M.A. Abu el Maaty, J. Song, C. Yu, J. Zhou, K. Han, H. Sun, A. Casini, I. Ott, S. Wölfl, J. Med. Chem. 66 (2023) 3995–4008;
(b) M. Hu, X.-L. Zhou, T.-X. Xiao, L. Hao, Y. Li, Dalton Trans. 52 (2023) 15859–15865;
(c) C. Huang, H. Zhang, Y. Yang, H. Liu, J. Chen, Y. Wang, L. Liang, H. Hu, Y. Liu, J. Inorg. Biochem. 247 (2023) 112329;
(d) S.S. Massoud, F.R. Louka, N.M.H. Salem, R.C. Fischer, A. Torvisco, F. A. Mautner, J. Vančo, J. Belza, Z. Dvořák, Z. Trávníček, Eur. J. Med. Chem. 246 (2023) 114992.
[54] O.V. Dolomanov, L.J. Bourhis, R.J. Gildea, J.A.K. Howard, H. Puschmann, OLEX2: a complete structure solution, refinement and analysis program, J. Appl. Crystallogr. 42 (2009) 339–341.